AD_____

Award Number: W81XWH-05-1-0300

TITLE: Structural Characterization and Determinants of Specificity of Single-Chain Antibody Inhibitors of Membrane-Type Serine Protease 1

PRINCIPAL INVESTIGATOR: Christopher J. Farady

CONTRACTING ORGANIZATION: University of California, San Francisco
San Francisco, CA 94143-2280

REPORT DATE: March 2008

TYPE OF REPORT: Annual Summary

PREPARED FOR: U.S. Army Medical Research and Materiel Command
Fort Detrick, Maryland 21702-5012

REPORT DOCUMENTATION PAGE

Form Approved
OMB No. 0704-0188

1. REPORT DATE *(DD-MM-YYYY)*	**2. REPORT TYPE**	**3. DATES COVERED** *(From - To)*
01-03-2008	Annual Summary	21 FEB 2005 - 20 FEB 2008

4. TITLE AND SUBTITLE

Structural Characterization and Determinants of Specificity of Single-Chain Antibody Inhibitors of Membrane-Type Serine Protease 1

5a. CONTRACT NUMBER

5b. GRANT NUMBER
W81XWH-05-1-0300

5c. PROGRAM ELEMENT NUMBER

6. AUTHOR(S)
Christopher J. Farady

E-Mail: christopher.farady@ucsf.edu

5d. PROJECT NUMBER

5e. TASK NUMBER

5f. WORK UNIT NUMBER

7. PERFORMING ORGANIZATION NAME(S) AND ADDRESS(ES)

8. PERFORMING ORGANIZATION REPORT NUMBER

9. SPONSORING / MONITORING AGENCY NAME(S) AND ADDRESS(ES)
U.S. Army Medical Research and Materiel Command
Fort Detrick, Maryland 21702-5012

10. SPONSOR/MONITOR'S ACRONYM(S)

11. SPONSOR/MONITOR'S REPORT NUMBER(S)

12. DISTRIBUTION / AVAILABILITY STATEMENT
Approved for Public Release; Distribution Unlimited

13. SUPPLEMENTARY NOTES

14. ABSTRACT

Membrane-type serine protease 1 (MT-SP1) is a cancer-associated serine protease implicated in the tumorogenesis and metastasis of breast cancer. Inhibition of MT-SP1 activity has been shown to decrease metastatic potential. We have developed a number of potent and specific single-chain (scFv) antibody inhibitors to MT-SP1, and have begun to characterize their mechanism of inhibition. Through kinetic characterization and site-directed mutagenesis experiments, it has been determined that three potent inhibitors have separate and novel mechanisms of inhibition which do not mimic either biologically or pharmaceutically relevant protease inhibitors. These novel modes of binding and inhibition are the basis for their specificity, and suggest these inhibitors will have less cross-reactivity and toxicity problems when used *in vivo* to further dissect the role of MT-SP1 in breast cancer.

15. SUBJECT TERMS
Antibody inhibitors, Proteases in cancer, Protease specificity

16. SECURITY CLASSIFICATION OF:			**17. LIMITATION OF ABSTRACT**	**18. NUMBER OF PAGES**	**19a. NAME OF RESPONSIBLE PERSON**
a. REPORT	**b. ABSTRACT**	**c. THIS PAGE**			USAMRMC
U	U	U	UU	35	**19b. TELEPHONE NUMBER** *(include area code)*

Table of Contents

Introduction…….…… 4

Body…… 5-6

Key Research Accomplishments…….……. 6

Reportable Outcomes…… 6

References…….. 7

Appendix 1……..... 8-36

Introduction:

My research has focused on the mechanism of inhibition of a set of single-chain inhibitors of Membrane-Type Serine Protease 1 (MT-SP1). MT-SP1 is a type II transmembrane serine protease (TTSP) expressed on the surface of epithelial cells. Research over the past 10 years have shown that MT-SP1 is involved in a number of biological processes, including tissue development, cell adhesion, and growth factor activation. Furthermore, a number of experiments have suggested dysregulated MT-SP1 activity may have a critical role in tumor progression and metastasis [1]. Immunoblotting, immunohistochemical analysis, and expression level analysis have found MT-SP1 to be differentially overexpressed in breast, prostate, and ovarian cancers. MT-SP1 has been shown to play a role in ovarian [2] and prostate [3] tumor invasion using experimental methods including inhibition of MT-SP1 by small molecules and anti-sense. In breast cancer, MT-SP1 expression levels, when correlated with substrate expression levels have been prognostic in disease progression. High levels of MT-SP1 expression has been correlated with the expression of hepatocyte growth factor (HGF) and the Met/HGF receptor [4], and with the glycosylation enzyme β1,6-N-Acetylglucosaminyltransferase V [5], and in both cases, these clusters showed prognostic value for disease-related survival. MT-SP1 expression levels have also been correlated with macrophage stimulating protein (MSP) [6], and co-expression of MT-SP1, MSP, and its receptor, RON, have been implicated in breast cancer metastasis to the bone [7]. Finally, modest orthotopic overexpression of MT-SP1 in mouse epidermal tissue led to spontaneous squamous cell carcinomas [8], further cementing MT-SP1's role in cancer, and suggesting the enzyme is causally involved in malignant transformation.

In order to tease apart the role of MT-SP1 in tumor progression, the Craik Lab has used phage display to develop a series of potent and specific single-chain antibody inhibitors (scFv) of the catalytic domain of MT-SP1 [9]. With K_i's ranging from 10pM to 10nM, these inhibitors are extremely potent *in vitro*, and showed no appreciable inhibition of a panel of closely related serine proteases including factor Xa, thrombin, kallikrein, tPA, and uPA. The potential benefits of these inhibitors are two-fold: they can be used to probe complex biology of MT-SP1, both its role in normal and cancer biology, and they can be used to validate MT-SP1 as both an imaging and therapeutic target. From a more biophysical standpoint, these inhibitors are unique in that they are the only reported antibody inhibitors of serine proteases, a large class of homologous enzymes in which the development of specific inhibitors has been a monumental challenge. Most protease inhibitors take advantage of either the catalytic machinery or topological fold of the protease. These scFv inhibitors bind and recognize a specific three-dimensional epitope near the active site of the enzyme, which allows for specificity among proteases, and allows for a fundamentally different mechanism of inhibition from other biologically active protease inhibitors. A thorough understanding of the mechanism of inhibition of these inhibitors will help us validate their putative mode of action *in vivo*, and will suggest new strategies for inhibition of MT-SP1 and other serine proteases.

Results:

During the duration of this grant, the majority of my aims, to structurally and biochemically characterize novel antibody-based inhibitors of the breast cancer associated serine protease MT-SP1, have been met. Previously, we determined the mechanism of inhibition of the two most potent inhibitors. These results were summarized in 2007 annual report and published last year [10]. In the past 12 months, we have solved the crystal structure of the E2 / MT-SP1 complex, which has given us insight into how exactly this inhibitor binds to and inhibits the protease. These results have recently been published in the *Journal of Molecular Biology* and are attached in appendix 1.

To get the protease/inhibitor complex to crystallize, it was necessary to convert the scFv antibody construct to an Fab. The protease/inhibitor complex was then successfully crystallized, and the structure was determined to 2.2 Å resolution. The structure revealed the basis of E2's potency and specificity. The inhibitor has a novel mechanism of inhibition; it gains potency and specificity through interactions with the protease surface loops, and inhibits by binding in the active site in a catalytically non-competent manner. The antibody caps the protease active site and the interaction has a large buried surface area, which is responsible for much of the potency. Verifying our mutational data, E2 does indeed make significant contacts with the MT-SP1 surface loops, and as these are areas of high diversity among serine proteases, these contacts are responsible for the antibody specificity. E2 inhibits MT-SP1 by inserting its very long H3 loop in the protease active site. It binds in such a manner so that the peptide cannot approach the catalytic residue and be cut.

The significance of these results are two-fold. The mechanisms of inhibition provide a rationale for the effectiveness of these inhibitors, and suggest that the development of specific antibody-based inhibitors against individual members of closely related enzyme families is feasible, and an effective way to develop tools to tease apart complex biological processes. This structure was only the second structure of a protease/inhibitory antibody complex, and revealed that, in contrast to most naturally occurring protease inhibitors, which have diverse structures but converge to a similar inhibitory archetype, antibody inhibitors provide an opportunity to develop divergent mechanisms of inhibition from a single scaffold. The inhibitors might also be effective *in vivo* tools, either as biological inhibitors of MT-SP1, or as imaging or detection tools. E2 has been used as a tool to validate the growth factor MSP as a substrate of MT-SP1, and is being used in imaging experiments to detect breast cancer tumors in mice, which are being performed by collaborators at UCSF.

Future Directions

Though the term of this fellowship is finished, we are still interested in pursuing the structure of the S4 antibody in complex with MT-SP1, to complete the research proposed. The inhibitor will likely have a different inhibitory motif, which should help us better understand how antibodies can be engineered to specifically and potently inhibit cancer related serine proteases.

Key Research and Training Accomplishments:

- Determined the structure and mechanism of inhibition of the most potent antibody inhibitor of the breast-cancer associated serine protease MT-SP1. These results have been summarized in the manuscript "Structure of an Fab-Protease Complex Reveals A Highly Specific Non-Canonical Mechanism of Inhibition", which has been accepted by the *Journal of Molecular Biology* (see Reportable Outcomes and Appendix 1).

- Converted the E2 scFv to an Fab scaffold. Having multiple constructs of the antibodies gives us flexibility when we use these inhibitors in future *in vivo* experiments.

- Will finish my doctorate in May, 2008.

Reportable Outcomes:

One paper has been published in the past year

- Farady, CJ, Egea, PF, Schneider EL, Darragh, MR, Craik, CS. Structure of an Fab-Protease Complex Reveals A Highly Specific Non-Canonical Mechanism of Inhibition. (2008) *J Mol Biol. In press*

Previously, two papers were published on this work

- Bhatt, AS, Welm, A, Farady, CJ, Vasquez, M, Wilson, K, and Craik, CS. (2007). Coordinate expression and functional profiling identify an extracellular proteolytic signaling pathway. *Proc Natl Acad Sci U S A* **104**, 5771-5776.
- Farady, CJ, Sun, J, Darragh, MR, Miller, SM, and Craik, CS. (2007). The mechanism of inhibition of antibody-based inhibitors of Membrane-Type Serine Protease 1 (MT-SP1). *J Mol Biol* **369**, 1041-51.

This work was also presented at the following conferences:

- Attended and gave a poster presentation at the 2007 UCSF Breast Oncology Program annual conference
- Attended and gave an oral presentation at the International Proteolysis Society conference in October, 2007

References

1. Uhland, K., *Matriptase and its putative role in cancer*. Cell Mol Life Sci, 2006. **63**(24): p. 2968-78.
2. Suzuki, M., et al., *Inhibition of tumor invasion by genomic down-regulation of matriptase through suppression of activation of receptor-bound pro-urokinase*. J Biol Chem, 2004. **279**(15): p. 14899-908.
3. Galkin, A.V., et al., *CVS-3983, a selective matriptase inhibitor, suppresses the growth of androgen independent prostate tumor xenografts*. Prostate, 2004. **61**(3): p. 228-35.
4. Kang, J.Y., et al., *Tissue microarray analysis of hepatocyte growth factor/Met pathway components reveals a role for Met, matriptase, and hepatocyte growth factor activator inhibitor 1 in the progression of node-negative breast cancer*. Cancer Res, 2003. **63**(5): p. 1101-5.
5. Siddiqui, S.F., et al., *Coexpression of beta1,6-N-acetylglucosaminyltransferase V glycoprotein substrates defines aggressive breast cancers with poor outcome*. Cancer Epidemiol Biomarkers Prev, 2005. **14**(11 Pt 1): p. 2517-23.
6. Bhatt, A.S., et al., *Coordinate expression and functional profiling identify an extracellular proteolytic signaling pathway*. Proc Natl Acad Sci U S A, 2007. **104**(14): p. 5771-6.
7. Welm, A.L., et al., *The macrophage-stimulating protein pathway promotes metastasis in a mouse model for breast cancer and predicts poor prognosis in humans*. Proc Natl Acad Sci U S A, 2007. **104**(18): p. 7570-5.
8. List, K., et al., *Deregulated matriptase causes ras-independent multistage carcinogenesis and promotes ras-mediated malignant transformation*. Genes Dev, 2005. **19**(16): p. 1934-50.
9. Sun, J., J. Pons, and C.S. Craik, *Potent and selective inhibition of membrane-type serine protease 1 by human single-chain antibodies*. Biochemistry, 2003. **42**(4): p. 892-900.
10. Farady, C.J., et al., *The mechanism of inhibition of antibody-based inhibitors of membrane-type serine protease 1 (MT-SP1)*. J Mol Biol, 2007. **369**(4): p. 1041-51.

Elsevier Editorial System(tm) for Journal of Molecular Biology

Manuscript Draft

Manuscript Number: JMB-D-08-00475R1

Title: Structure of an Fab-protease complex reveals a highly specific non-canonical mechanism of inhibition

Article Type: Full Length Article

Section/Category: Protein and nucleic acid structure, function, and interactions

Keywords: antibody; serine protease; protease inhibitor; substrate specificity; structure

Corresponding Author: Professor Charles Craik,

Corresponding Author's Institution: University of California, San Francisco

First Author: Christopher J Farady

Order of Authors: Christopher J Farady; Pascal F Egea; Eric L Schneider; Molly R Darragh; Charles Craik

Manuscript Region of Origin:

Abstract: The vast majority of protein protease inhibitors bind their targets in a substrate-like manner. This is a robust and efficient mechanism of inhibition, but due to the highly conserved architecture of protease active sites, these inhibitors often exhibit promiscuity. Inhibitors that show strict specificity for one protease usually achieve this selectivity by combining substrate-like binding in the active site with exosite binding on the protease surface. The development of new, specific inhibitors can be greatly aided by binding to non-conserved regions of proteases if potency can be maintained. Due to their ability to bind specifically to nearly any antigen, antibodies provide an excellent scaffold for creating inhibitors targeted to a single member of a family of highly homologous enzymes. The 2.2 Å resolution crystal structure of an Fab antibody inhibitor in complex with the serine protease membrane-type serine protease 1 (MT-SP1/matriptase) reveals the molecular basis of its picomolar potency and specificity. The inhibitor has a distinct mechanism of inhibition; it gains potency and specificity through interactions with the protease surface loops, and inhibits by binding in the active site in a catalytically non-competent manner. In contrast to most naturally occurring protease inhibitors, which have diverse structures but converge to a similar inhibitory archetype, antibody inhibitors provide an opportunity to develop divergent mechanisms of inhibition from a single scaffold.

Structure of an Fab-protease complex reveals a highly specific non-canonical mechanism of inhibition

Christopher J. Farady[1], Pascal F. Egea[3], Eric L. Schneider[2], Molly R. Darragh[1], and Charles S. Craik[1,2#].

[1]Graduate Group in Biophysics, University of California, San Francisco, 600 16th St. Genentech Hall, San Francisco, CA. 94143-2240, USA.
[2]Department of Pharmaceutical Chemistry, University of California, San Francisco, 600 16th St. Genentech Hall, San Francisco, CA. 94143-2280, USA.
[3]Department of Biochemistry and Biophysics, University of California, San Francisco, 600 16th St. Genentech Hall, San Francisco, CA. 94143-2240, USA.
Corresponding Author

Summary

The vast majority of protein protease inhibitors bind their targets in a substrate-like manner. This is a robust and efficient mechanism of inhibition, but due to the highly conserved architecture of protease active sites, these inhibitors often exhibit promiscuity. Inhibitors that show strict specificity for one protease usually achieve this selectivity by combining substrate-like binding in the active site with exosite binding on the protease surface. The development of new, specific inhibitors can be greatly aided by binding to non-conserved regions of proteases if potency can be maintained. Due to their ability to bind specifically to nearly any antigen, antibodies provide an excellent scaffold for creating inhibitors targeted to a single member of a family of highly homologous enzymes. The 2.2 Å resolution crystal structure of an Fab antibody inhibitor in complex with the serine protease membrane-type serine protease 1 (MT-SP1/matriptase) reveals the molecular basis of its picomolar potency and specificity. The inhibitor has a distinct mechanism of inhibition; it gains potency and specificity through interactions with the protease surface loops, and inhibits by binding in the active site in a catalytically non-competent manner. In contrast to most naturally occurring protease inhibitors, which have diverse structures but converge to a similar inhibitory archetype, antibody inhibitors provide an opportunity to develop divergent mechanisms of inhibition from a single scaffold.

Keywords: antibody, serine protease, protease inhibitor, substrate specificity, structure.

Introduction

Proteolytic activity *in vivo* is carefully regulated by spatial and temporal localization, zymogen activation, autolysis, and through the inhibition of proteases by macromolecular inhibitors. Despite divergent targets and different mechanisms of inhibition, most protease inhibitors bind a critical portion of the inhibitor in the active site in a substrate-like manner. Though an effective paradigm for protease inhibition, substrate-like binding in the active site often leads to inhibitors that can potently inhibit more than one target protease. This promiscuity is evidenced by the fact that 115 annotated human protease inhibitors are capable of regulating the activity of the 612 known human proteases[1]. The few specific protease inhibitors found in biology, such as rhodniin, a thrombin inhibitor from *Rhodnius prolixus*, have gained specificity by combining substrate-like inhibition with exosite binding. Rhodniin has two domains, one of which binds and inhibits the protease via a canonical mechanism, and a second domain evolved to bind to exosite I, resulting in a potent and specific thrombin inhibitor[2].

Dysregulated proteolytic activity plays a role in many disease states, often caused by a single member of highly homologous protease families. As such, there is a need for selective inhibitors. Traditional attempts to develop small molecule or protein protease inhibitors have had mixed results[3,4]; difficulties have primarily been due to specificity issues arising from the similarity of protease active sites. Therefore, there is a need for more diverse methods for developing specific inhibitors to single members of these highly similar enzymes.

Due to their ability to selectively bind closely related antigens, antibodies provide a particularly attractive scaffold on which to develop specific enzyme inhibitors. Of the antibody-based protease inhibitors which have been reported in the literature[5; 6; 7; 8; 9; 10; 11], most work by interfering with protein-

protein interaction sites rather than interacting with the active site of the enzyme. Previously, we used a phage-displayed single chain antibody library to develop potent and specific inhibitors of membrane type serine protease 1 (MT-SP1/matriptase), but the molecular details of the inhibitory mechanism remained unclear[12; 13]. MT-SP1 is a cell-anchored serine protease involved in cell signaling pathways and protease activation, and has been implicated in cancer progression[14; 15; 16]. It is a member of a large family of closely related enzymes, the trypsin-fold serine proteases. Here we report the crystal structure at 2.2 Å resolution of E2, the most potent previously described antibody inhibitor, in complex with the catalytic domain of MT-SP1. E2 has a distinct mechanism of inhibition; it gains potency and specificity through interactions with the protease surface loops, and binds in the active site in a catalytically non-competent manner.

Results

Characterization of Inhibitory Fab

E2 was raised from a phage-displayed fully synthetic human combinatorial scFv library with modular consensus frameworks and randomized CDR3s as previously described[17]. We have reported the biochemical characterization of E2[13], but the scFv construct proved unsuitable for structural studies, so the Fv was transferred to an Fab scaffold by ligating the variable region to a human Fab constant region[18]. The conversion from an scFv to Fab scaffold had minimal effect on the inhibitory potency of the antibody, which had a K_I of 15 pM against MT-SP1 (data not shown).

E2/MT-SP1 Structure

The E2/MT-SP1 structure was determined to 2.2 Å, with two copies of the complex in the asymmetric unit. The antibody caps the protease active site and makes numerous interactions with the surface loops

of the protease (Figure 1). These loops surround the substrate-binding groove of the protease, modulate macromolecular substrate recognition, and are sites of high diversity among the well-conserved family of trypsin-like serine proteases[19]. The Fv heavy chain packs against the 60's and 90's loop (standard chymotrypsinogen numbering) while the light chain interacts with the 170's and 220's loop on the opposite side of the protease (Figure 1, Table 1). The E2 light chain makes very few interactions with MT-SP1, burying only 175 $Å^2$, or about 15% of the total buried surface area of the Fab-protease interaction.

The antibody hypervariable loops bind to the protease surface loops by either packing against them or by "grabbing" the loop by stacking it between two CDR loops. This "grabbing" phenomenon is seen most clearly in the antibody's interaction with the 90's loop of MT-SP1, which is stacked between the hypervariable H2 and H3 loops (Figure 2(a)). The 90's loop buries the Phe97 side chain in the hydrophobic core of the antibody hypervariable region, where it is stacked between H2 residue TyrH58 (Kabat numbering) and the AsnH100g side chain of H3. These two crucial interactions alone bury 145 $Å^2$ of surface area (Table 1). In the apo MT-SP1 structure[20], Asp96 forms the bottom of the S4 pocket, allowing a positively charged substrate P4 residue. In the antibody structure, however, Asp96 is rotated 180 degrees around the side chain Cβ, allowing it to interact with the Fab H2. This rotation allows the Asp96 carboxylic acid moiety to H-bond to the backbone amide of SerH53 (2.8 Å) and the side chain Oγ atoms of SerH53 and SerH56. The 170's loop is also "grabbed" by E2. It is bound between the L1 loop, which makes van der Waals contacts with the protease Pro173, the L3 loop, which makes an H-bond between AsnL93 Oδ2 and the protease Gln174 side chain, and H3 residues AsnH100g and ValH100h, which make an H-bond to Gln174 Oε1 and van der Waals contacts with Gln175, respectively.

The most striking feature of the E2 structure is the extended binding conformation of the CDR H3 loop in the protease active site (Figure 2(b)). E2 has a long 18-residue H3 loop, which bridges the active site and buries 847 $Å^2$ of surface area, about 68% of the total buried surface area of the Fab-protease interaction. Though lacking secondary structure, the loop is rigidified by the presence of four prolines. The N-terminus of the loop bends over and packs against the 140's loop, which regulates the approach of H3 towards the active site. The protease Tyr146 side chain is stacked between the antibody side chains TyrH99 and GlnH100a, and the Tyr146 OH residue forms H-bonds with the backbone nitrogens of ProH100 and GlnH100a, at 3.1 Å and 2.9 Å, respectively (Figure 3). As the H3 loop approaches the catalytic residues, it inserts the first of two arginines* (ArgH100b) in the S1 pocket. The H3 loop then makes a sharp turn, allowing the side chain of the second arginine (ArgH100c) to extend into the prime side of the active site. The next two residues, P2' and P3', bind in the S2 and S3 pockets, respectively, before bending up and back out of the active site (Figure 2(b)). The P2' and P3' residues are GlyH100d and ProH100e, respectively, and though they bind in the substrate pockets, they do not bind in a substrate like manner, as the chloromethyl ketone inhibitor D-FPR-cmk binds in the fVIIa active site[21]. They are oriented slightly above D-FPR-cmk, and do not extend side chains into the binding pockets (Figure 4(a)). We previously showed that E2 could be processed between the two arginine residues when incubated with MT-SP1 at pH 6.0 for an extended period of time. This is a hallmark of standard mechanism serine protease inhibitors, and suggested that the inhibitor bound in some sort of substrate-like manner. In light of the structure, it is clear that E2 is in fact an extremely poor substrate due to the 7.5 Å distance between the catalytic Ser195 Oγ and the carbonyl carbon of the scissile bond (defined as

*The scFv residues corresponding to ArgH100b and ArgH100c were previously[13] referred to as Arg131 and Arg132, respectively.

the peptide bond in closest proximity to Ser195) and can only be cleaved when the complex is compromised at low pH[22].

The ArgH100b side chain of E2 binds in the S1 pocket of MT-SP1 in an unexpected manner (Figure 2(c)). The NH2 makes a 3.1 Å hydrogen bond to Ser190 Oγ and a 2.9 Å water-mediated hydrogen bond to Asp189 Oδ1 at the base of the S1 pocket. This is similar to the binding mode of the terminal amine of Lys15 of BPTI, but different than that of benzamidine[20], an inhibitor which mimics arginine-binding in the S1 pocket by making a salt bridge interaction with Asp189 (Figure 2(c)). P1 arginine binding in the S1 pocket is thus sub-optimal. The side chain – and by extension the scissile bond – are restricted from binding more deeply in the active site due to the geometric constraints placed upon them by the orientation of the H3 loop.

E2 Preferentially Binds to the Active Form of MT-SP1

The significant interactions E2 makes with the protease active site have another benefit. E2 interacts with the 220's loop, 140's loop, and in the S1 pocket. These residues are all part of the activation domain of trypsin-fold serine proteases, which become ordered upon zymogen activation[23]. Surface plasmon resonance shows that E2 does not bind to the zymogen form of the enzyme (Figure 6). At 500 nM, the zymogen does not bind to immobilized E2, while the active protease gives a robust binding signal. A K_D for the zymogen could not be determined as the zymogen could not be concentrated enough to see binding. E2 can thus preferentially bind to the active form of the protease, further showing that antibody inhibitors can be specific enough to target distinct conformations of a single enzyme.

Discussion

The structure of the antibody-based inhibitor E2 in complex with the serine protease MT-SP1 reveals the basis of its potency and specificity. In contrast to the vast majority of naturally-occurring protein protease inhibitors, which primarily bind in the protease active site, this antibody-based inhibitor binds to the surface loops flanking the protease active site. The sequences and conformations of these loops are highly degenerate among families of proteases, and thus they are sites of natural diversity. This is analogous to naturally occurring inhibitors that show a high degree of specificity, such as anti-coagulation inhibitors from blood-meal parasites, which gain selectivity by binding to exosites on the surface of the protease. But while relatively few protease exosites have been discovered, the diversity of protease surface loops makes them attractive areas to target to build specificity into an inhibitor.

The potency of E2 is striking, and our structure reveals why; the inhibitor buries a large surface area, and the antibody scaffold orients the inhibitor H3 loop in a non-substrate-like conformation in the active site to inhibit the protease. The canonical serine protease inhibitor BPTI inhibits trypsin with a K_I of 0.6 pM[24]; a potency that arises from exquisite shape and charge complementarity between enzyme and inhibitor[25]. In contrast, these inhibitors bind in a sub-optimal manner in the active site. E2 does not make an energetically favored salt bridge with Asp189 in the S1 pocket of the protease, and though it makes significant contacts with other protease subsites, they are not optimal. The P2' and P3' residues are glycine and proline respectively, and make only modest backbone interactions with the protease (Figure 4(a)). Despite this, E2 has a K_I in the low picomolar range. Active site binding is responsible for some of this binding energy – the ArgH100b binding in the S1 pocket provides 5 kcal/mol binding energy for E2[13] - but the many interactions with the surface loops are critical as well. The 1241 Å^2 of surface area that E2 buries on MT-SP1 is larger than the typical antibody/ protein antigen interaction, which averages about 875 Å^2 [26; 27]. This interaction area is also large for a protease inhibitor; TIMP

inhibitors bury a similar surface area on matrix metalloproteases[28], while stefin inhibitors of cysteine proteases [29] and canonical serine protease inhibitors[30] have interfaces of about 900 Å^2. Much effort has gone into using phage display and rational design to impart selectivity onto naturally occurring protease inhibitors[31; 32]. This is difficult, since standard mechanism inhibitors have been evolved for maximum inhibitory efficiency. Some of this potency has to be sacrificed for these inhibitors to gain specificity. But with protein scaffolds engineered to be protease inhibitors, potency and specificity are necessarily linked. If a protein can be engineered to bind to a large surface area and interfere with the catalytic machinery of an enzyme, it will most likely be specific.

A number of macromolecular MT-SP1 inhibitors have been described, all of which bind in the active site in a substrate like manner[20; 33; 34; 35]. Using the structural and kinetic data presented here, we can describe a broader 'inhibitope' for MT-SP1, a set of crucial contacts and interactions that, when linked together on the correct scaffold, lead to potent and specific inhibition. For E2, maximal MT-SP1 inhibition depends on interactions with the 90's loop, 140's loop, an arginine side chain in the S1 pocket, and non-substrate-like binding in the protease active site. Inhibitors of the closely related protease urokinase plasminogen activator (uPA) have a different inhibitope. Cyclic peptide uPA inhibitors have a strict requirement for an arginine P1[36], but anti-uPA mAb's[9] make many more significant interactions with the 37's and 60's loops of uPA, on the prime-side of the protease active site, suggesting these loops provide possible anchor points for inhibition.

Recently, the structures of two inhibitory antibodies of the serine protease hepatocyte growth factor activator (HGFA) were reported[37]. One inhibitor, Ab75, appeared to be an allosteric inhibitor, while the most potent inhibitor, Ab58, had some similarities to E2 inhibition of MT-SP1. Ab58 buries the Phe97

residue of HGFA between two hypervariable loops, and uses the 90's loop as an anchor point, but binds to and inhibits the protease very differently. While E2 caps the MT-SP1 active site, Ab58 approaches the active site at an angle (Figure 5(a)). The H1 and H2 loops of Ab58 are located in the substrate-binding groove, but the inhibitors do not approach the S1 pocket or the catalytic residues (Figure 5(b)). A similar mechanism of inhibition would probably not be possible for MT-SP1, which has a deeper and more occluded active site cleft than HGFA. Thus, using a similar antibody scaffold it is possible to develop specific protease inhibitors with completely novel mechanisms of inhibition. Whether aspects of these inhibitopes and mechanisms can guide the rational design of new inhibitors is yet to be seen, but given an appropriate scaffold, an antigen with a three-dimensional epitope, and an inhibitor library with sufficient diversity, it should be possible to develop specific inhibitors with novel mechanisms of action.

The structure presented here helps define the mechanism of inhibition of a potent and specific antibody inhibitor of a serine protease. The mechanism was unexpected. It would be difficult to predict which protease residues or loops would be amenable to binding, or that the H3 loop would be able to adopt a non-substrate-like conformation in the active site that would allow for potent inhibition of MT-SP1. By utilizing robust binding scaffolds and combinatorial selection techniques to identify unique inhibitopes, we have developed selective inhibitors with mechanisms that are specific for MT-SP1. This provides the opportunity to develop potent and selective inhibitors against individual enzymes, and precisely monitor and modulate a wide array of proteolytic processes.

Materials and Methods

Protein Expression, purification, and mutagenesis

MT-SP1 and its mutants were expressed in *Escherichia coli* and purified as previously described[13; 38]. The zymogen was created by an R15A substitution, which prevented protease activation. It elutes from a gel filtration column at the same time as the active protease, but shows no enzymatic activity. For crystallization purposes, the surface Cys122 residue was mutated to serine using the Stratagene Quickchange kit (Stratagene, La Jolla, CA). The E2 scFv was converted to an Fab by using overlap extension PCR[39] between the scFv and the humanized constant region from the Fab phage displayed library. The overlapped region corresponded to residues 104-113 in the heavy chain and 98-107 in the light chain. It was verified by DNA sequencing, expressed in *E coli*, and purified as previously described [12].

Steady State Kinetics

Kinetics were carried out as previously described[13]. Briefly, reactions were carried out in 50 mM Tris, pH 8.8, 50 mM NaCl, 0.01% Tween-20 in 96-well, medium binding, flat-bottomed plate (Corning), and cleavage of substrate (Spectrazyme-tPA (hexahydrotyrosyl-Gly-Arg-pNA), American Diagnostica, Greenwich, CT) was monitored in a UVmax Microplate Reader (Molecular Devices Corporation, Palo Alto, CA.). K_I's were measured using the tight-binding inhibition equations of Williams and Morrison[40]. All graphs and equations were fit using Kaleidagraph 3.6 (Synergy Software, Reading, PA).

Surface Plasmon Resonance.

The association and dissociation curves for MT-SP1 and the inactive zymogen MT-SP1 R15A were obtained by surface plasmon resonance using a BIAcore Biosensor T100 (GE Healthcare). The E2 Fab (ligand), in 25 mM sodium acetate buffer, pH=5.0, was covalently immobilized onto a CM5 chip according to the manufacturer's protocol with a final immobilization level of ~120 RU. The reference

channel was treated using the same chemistry as the ligand coupled surface. Enzymes (analytes) were washed in HBS-EP buffer (10 mM HEPES pH=7.4, 150 mM NaCl, 3 mM EDTA and 0.005% [v/v] Tween 20) and injected in varying concentrations (0.4-400 nM for MT-SP1, 100 nM-20 μM for MT-SP1 R15A) across the chip surface at 25 μL/min. Surface regenerations were performed with 100 mM Glycine pH=2.2, allowing a complete return to baseline. The sensorgram of the reference surface was subtracted from the ligand-conjugated surface for each injection. Multiple injections of HBS-EP were also used to remove noise from the data.

Crystallization and Data Collection

E2 was incubated with MT-SP1 in 1:1 molar ratio, the complexes were purified by gel filtration in a buffer containing 50 mM Tris pH8.0, 100 mM NaCl, 5% glycerol, and then concentrated to 15-20 mg/ml. High-throughput crystallization screening was performed using a nanoliter-scale Mosquito robot (TTP Labtech) in hanging drops by vapor diffusion. The E2/MT-SP1 complex crystallized in 16% PEG 5000 MME, 0.21 M $AmSO_4$ and 0.1 M Tris pH8.0. Crystals belonging to the orthorhombic space group $P2_12_12_1$ (a=48.63Å, b=163.28 Å and c=201.16 Å) grew in two days, and were cryoprotected in the mother liquor supplemented with 20% ethylene glycol. Diffraction data were collected at beamline 8.3.1 at the Advanced Light Source at LBNL. E2/MT-SP1 data were reduced and scaled using Elves[41].

Structure determination and refinement.

The structure was solved by molecular replacement using Phaser[42] in CCP4[43], first searching for MT-SP1 (using 1EAX as search model), then searching for the Fab fragment with its H3 loop truncated (using 2HFF as search model) for the MT-SP1 complex. Molecular replacement was followed by automatic building in ARP/wARP[44] and manual building cycles. Restrained refinement cycles were

done using Phenix[45] and TLS refinement was applied in the last stages of the refinement. Fab residues 127-137 and 186-192 of heavy chain D and 127-131 of heavy chain F had no density, and were left out of the refinement model. These regions are often disordered in Fab structures, and make no interactions with the protease. Furthermore, light chain E residues LysH145, LysH190, AsnH210, light chain C residues LysH190 and PheH209, heavy chain D residues LysH209, LysH210, and LysH214, and heavy chain F residue ThrH191 and LysH214 had no side chain density and were truncated at Cβ.

For both structures, analysis of the thermal motion parameters with TLSMD (http://skuld.bmsc.washington.edu/~tlsmd/) revealed anisotropic motions between the constant and variable regions for the complexes present in the asymmetric unit. The proteases were treated as single groups and antibody chains were treated as two separate groups with the boundary defined at the hinge between the constant and variable regions. The quality of the final structure was assessed using Molprobity[46]. Buried surface area calculations were performed using PISA[27].

Accession Codes:

Coordinates and structure factors have been deposited at the Protein Data Bank (code 3BN9).

Acknowledgements:

The authors would like to thank Professor Robert Fletterick for critical reading of the manuscript, Dr. James Holton and Dr. George Meigs for assistance at ALS beamline 8.3.1, and Jeremy Wilbur and Dr. Peter Hwang for technical assistance with the Biacore. This work was funded by NIH grants CA072006 and GM082250 (C.S.C), Department of Defense grant BC043431 (C.J.F), and an NSF graduate research fellowship (MRD).

References

1. Rawlings, N. D., Morton, F. R. & Barrett, A. J. (2006). MEROPS: the peptidase database. *Nucleic Acids Res* **34**, D270-2.
2. Roussel, A., Mathieu, M., Dobbs, A., Luu, B., Cambillau, C. & Kellenberger, C. (2001). Complexation of two proteic insect inhibitors to the active site of chymotrypsin suggests decoupled roles for binding and selectivity. *J Biol Chem* **276**, 38893-8.
3. Coussens, L. M., Fingleton, B. & Matrisian, L. M. (2002). Matrix metalloproteinase inhibitors and cancer: trials and tribulations. *Science* **295**, 2387-92.
4. Turk, B. (2006). Targeting proteases: successes, failures and future prospects. *Nat Rev Drug Discov* **5**, 785-99.
5. Rezacova, P., Lescar, J., Brynda, J., Fabry, M., Horejsi, M., Sedlacek, J. & Bentley, G. A. (2001). Structural basis of HIV-1 and HIV-2 protease inhibition by a monoclonal antibody. *Structure* **9**, 887-95.
6. Puchi, M., Quinones, K., Concha, C., Iribarren, C., Bustos, P., Morin, V., Geneviere, A. M. & Imschenetzky, M. (2006). Microinjection of an antibody against the cysteine-protease involved in male chromatin remodeling blocks the development of sea urchin embryos at the initial cell cycle. *J Cell Biochem* **98**, 335-42.
7. Fukuoka, Y. & Schwartz, L. B. (2006). The B12 anti-tryptase monoclonal antibody disrupts the tetrameric structure of heparin-stabilized beta-tryptase to form monomers that are inactive at neutral pH and active at acidic pH. *J Immunol* **176**, 3165-72.
8. Matias-Roman, S., Galvez, B. G., Genis, L., Yanez-Mo, M., de la Rosa, G., Sanchez-Mateos, P., Sanchez-Madrid, F. & Arroyo, A. G. (2005). Membrane type 1-matrix metalloproteinase is involved in migration of human monocytes and is regulated through their interaction with fibronectin or endothelium. *Blood* **105**, 3956-64.
9. Petersen, H. H., Hansen, M., Schousboe, S. L. & Andreasen, P. A. (2001). Localization of epitopes for monoclonal antibodies to urokinase-type plasminogen activator: relationship between epitope localization and effects of antibodies on molecular interactions of the enzyme. *Eur J Biochem* **268**, 4430-9.
10. Xuan, J. A., Schneider, D., Toy, P., Lin, R., Newton, A., Zhu, Y., Finster, S., Vogel, D., Mintzer, B., Dinter, H., Light, D., Parry, R., Polokoff, M., Whitlow, M., Wu, Q. & Parry, G. (2006). Antibodies neutralizing hepsin protease activity do not impact cell growth but inhibit invasion of prostate and ovarian tumor cells in culture. *Cancer Res* **66**, 3611-9.
11. Obermajer, N., Premzl, A., Zavasnik Bergant, T., Turk, B. & Kos, J. (2006). Carboxypeptidase cathepsin X mediates beta2-integrin-dependent adhesion of differentiated U-937 cells. *Exp Cell Res* **312**, 2515-27.
12. Sun, J., Pons, J. & Craik, C. S. (2003). Potent and selective inhibition of membrane-type serine protease 1 by human single-chain antibodies. *Biochemistry* **42**, 892-900.
13. Farady, C. J., Sun, J., Darragh, M. R., Miller, S. M. & Craik, C. S. (2007). The mechanism of inhibition of antibody-based inhibitors of membrane-type serine protease 1 (MT-SP1). *J Mol Biol* **369**, 1041-51.

14. List, K., Szabo, R., Molinolo, A., Sriuranpong, V., Redeye, V., Murdock, T., Burke, B., Nielsen, B. S., Gutkind, J. S. & Bugge, T. H. (2005). Deregulated matriptase causes ras-independent multistage carcinogenesis and promotes ras-mediated malignant transformation. *Genes Dev* **19**, 1934-50.
15. Bhatt, A. S., Welm, A., Farady, C. J., Vasquez, M., Wilson, K. & Craik, C. S. (2007). Coordinate expression and functional profiling identify an extracellular proteolytic signaling pathway. *Proc Natl Acad Sci U S A* **104**, 5771-6.
16. Welm, A. L., Sneddon, J. B., Taylor, C., Nuyten, D. S., van de Vijver, M. J., Hasegawa, B. H. & Bishop, J. M. (2007). The macrophage-stimulating protein pathway promotes metastasis in a mouse model for breast cancer and predicts poor prognosis in humans. *Proc Natl Acad Sci U S A* **104**, 7570-5.
17. Knappik, A., Ge, L., Honegger, A., Pack, P., Fischer, M., Wellnhofer, G., Hoess, A., Wolle, J., Pluckthun, A. & Virnekas, B. (2000). Fully synthetic human combinatorial antibody libraries (HuCAL) based on modular consensus frameworks and CDRs randomized with trinucleotides. *J Mol Biol* **296**, 57-86.
18. de Haard, H. J., van Neer, N., Reurs, A., Hufton, S. E., Roovers, R. C., Henderikx, P., de Bruine, A. P., Arends, J. W. & Hoogenboom, H. R. (1999). A large non-immunized human Fab fragment phage library that permits rapid isolation and kinetic analysis of high affinity antibodies. *J Biol Chem* **274**, 18218-30.
19. Perona, J. J. & Craik, C. S. (1997). Evolutionary divergence of substrate specificity within the chymotrypsin-like serine protease fold. *J Biol Chem* **272**, 29987-90.
20. Friedrich, R., Fuentes-Prior, P., Ong, E., Coombs, G., Hunter, M., Oehler, R., Pierson, D., Gonzalez, R., Huber, R., Bode, W. & Madison, E. L. (2002). Catalytic domain structures of MT-SP1/matriptase, a matrix-degrading transmembrane serine proteinase. *J Biol Chem* **277**, 2160-8.
21. Bajaj, S. P., Schmidt, A. E., Agah, S., Bajaj, M. S. & Padmanabhan, K. (2006). High resolution structures of p-aminobenzamidine- and benzamidine-VIIa/soluble tissue factor: unpredicted conformation of the 192-193 peptide bond and mapping of Ca2+, Mg2+, Na+, and Zn2+ sites in factor VIIa. *J Biol Chem* **281**, 24873-88.
22. Luthy, J. A., Praissman, M., Finkenstadt, W. R. & Laskowski, M., Jr. (1973). Detailed mechanism of interaction of bovine -trypsin with soybean trypsin inhibitor (Kunitz). I. Stopped flow measurements. *J Biol Chem* **248**, 1760-71.
23. Bode, W., Schwager, P. & Huber, R. (1978). The transition of bovine trypsinogen to a trypsin-like state upon strong ligand binding. The refined crystal structures of the bovine trypsinogen-pancreatic trypsin inhibitor complex and of its ternary complex with Ile-Val at 1.9 A resolution. *J Mol Biol* **118**, 99-112.
24. Gebhard, W., Tschesche, T. & Fritz, H. (1986). Biochemistry of aprotinin and aprotinin-like inhibitors. In *Proteinase Inhibitors* (Barrett, A. J. & Salvesen, G., eds.), pp. p. 55-152. Elsevier, Amsterdam; New York.
25. Lawrence, M. C. & Colman, P. M. (1993). Shape complementarity at protein/protein interfaces. *J Mol Biol* **234**, 946-50.
26. Huang, M., Syed, R., Stura, E. A., Stone, M. J., Stefanko, R. S., Ruf, W., Edgington, T. S. & Wilson, I. A. (1998). The mechanism of an inhibitory antibody on TF-initiated blood coagulation revealed by the crystal structures of human tissue factor, Fab 5G9 and TF.G9 complex. *J Mol Biol* **275**, 873-94.
27. Krissinel, E. & Henrick, K. (2007). Inference of macromolecular assemblies from crystalline state. *J Mol Biol* **372**, 774-97.

28. Maskos, K., Lang, R., Tschesche, H. & Bode, W. (2007). Flexibility and variability of TIMP binding: X-ray structure of the complex between collagenase-3/MMP-13 and TIMP-2. *J Mol Biol* **366**, 1222-31.
29. Jenko, S., Dolenc, I., Guncar, G., Dobersek, A., Podobnik, M. & Turk, D. (2003). Crystal structure of Stefin A in complex with cathepsin H: N-terminal residues of inhibitors can adapt to the active sites of endo- and exopeptidases. *J Mol Biol* **326**, 875-85.
30. Scheidig, A. J., Hynes, T. R., Pelletier, L. A., Wells, J. A. & Kossiakoff, A. A. (1997). Crystal structures of bovine chymotrypsin and trypsin complexed to the inhibitor domain of Alzheimer's amyloid beta-protein precursor (APPI) and basic pancreatic trypsin inhibitor (BPTI): engineering of inhibitors with altered specificities. *Protein Sci* **6**, 1806-24.
31. Dennis, M. S. & Lazarus, R. A. (1994). Kunitz domain inhibitors of tissue factor-factor VIIa. II. Potent and specific inhibitors by competitive phage selection. *J Biol Chem* **269**, 22137-44.
32. Komiyama, T., VanderLugt, B., Fugere, M., Day, R., Kaufman, R. J. & Fuller, R. S. (2003). Optimization of protease-inhibitor interactions by randomizing adventitious contacts. *Proc Natl Acad Sci U S A* **100**, 8205-10.
33. Kirchhofer, D., Peek, M., Li, W., Stamos, J., Eigenbrot, C., Kadkhodayan, S., Elliott, J. M., Corpuz, R. T., Lazarus, R. A. & Moran, P. (2003). Tissue expression, protease specificity, and Kunitz domain functions of hepatocyte growth factor activator inhibitor-1B (HAI-1B), a new splice variant of HAI-1. *J Biol Chem* **278**, 36341-9.
34. Stoop, A. A. & Craik, C. S. (2003). Engineering of a macromolecular scaffold to develop specific protease inhibitors. *Nat Biotechnol* **21**, 1063-8.
35. Li, P., Jiang, S., Lee, S. L., Lin, C. Y., Johnson, M. D., Dickson, R. B., Michejda, C. J. & Roller, P. P. (2007). Design and Synthesis of Novel and Potent Inhibitors of the Type II Transmembrane Serine Protease, Matriptase, Based upon the Sunflower Trypsin Inhibitor-1. *J Med Chem* **50**, 5976-5983.
36. Zhao, G., Yuan, C., Wind, T., Huang, Z., Andreasen, P. A. & Huang, M. (2007). Structural basis of specificity of a peptidyl urokinase inhibitor, upain-1. *J Struct Biol* **160**, 1-10.
37. Wu, Y., Eigenbrot, C., Liang, W.-C., Stawicki, S., Shia, S., Fan, B., Ganesan, R., Lipari, M. T. & Kirchhofer, D. (2007). Structural insight into distinct mechanisms of protease inhibition by antibodies. *Proceedings of the National Academy of Sciences %R 10.1073/pnas.0708251104* **104**, 19784-19789.
38. Takeuchi, T., Shuman, M. A. & Craik, C. S. (1999). Reverse biochemistry: use of macromolecular protease inhibitors to dissect complex biological processes and identify a membrane-type serine protease in epithelial cancer and normal tissue. *Proc Natl Acad Sci U S A* **96**, 11054-61.
39. Ho, S. N., Hunt, H. D., Horton, R. M., Pullen, J. K. & Pease, L. R. (1989). Site-directed mutagenesis by overlap extension using the polymerase chain reaction. *Gene* **77**, 51-9.
40. Williams, J. W. & Morrison, J. F. (1979). The kinetics of reversible tight-binding inhibition. *Methods Enzymol* **63**, 437-67.
41. Holton, J. & Alber, T. (2004). Automated protein crystal structure determination using ELVES. *Proc Natl Acad Sci U S A* **101**, 1537-42.
42. Read, R. J. (2001). Pushing the boundaries of molecular replacement with maximum likelihood. *Acta Crystallogr D Biol Crystallogr* **57**, 1373-82.
43. (1994). The CCP4 suite: programs for protein crystallography. *Acta Crystallogr D Biol Crystallogr* **50**, 760-3.

44. Evrard, G. X., Langer, G. G., Perrakis, A. & Lamzin, V. S. (2007). Assessment of automatic ligand building in ARP/wARP. *Acta Crystallogr D Biol Crystallogr* **63**, 108-17.
45. Adams, P. D., Grosse-Kunstleve, R. W., Hung, L. W., Ioerger, T. R., McCoy, A. J., Moriarty, N. W., Read, R. J., Sacchettini, J. C., Sauter, N. K. & Terwilliger, T. C. (2002). PHENIX: building new software for automated crystallographic structure determination. *Acta Crystallogr D Biol Crystallogr* **58**, 1948-54.
46. Lovell, S. C., Davis, I. W., Arendall, W. B., 3rd, de Bakker, P. I., Word, J. M., Prisant, M. G., Richardson, J. S. & Richardson, D. C. (2003). Structure validation by Calpha geometry: phi,psi and Cbeta deviation. *Proteins* **50**, 437-50.

Figure Legends

Figure 1. Structure of the E2/MT-SP1 complex. The Fab (heavy chain, light blue; light chain, light red) caps MT-SP1 (grey) at the active site through interactions with the surface loops (green). H3 of E2 (dark blue) is inserted directly into the active site (catalytic triad indicated in yellow) while the remaining hypervariable loops (L1 and L2, pink; L3, red; H1 and H2, sky blue) interact with the protease surface loops. All figures were prepared using PyMoL [http://www.pymol.sourceforge.net].

Figure 2. Critical determinants of E2 (magenta) inhibition of MT-SP1 (gray). (*A*) The 90's (green) loop of MT-SP1 is bound between the H2 and H3 loops of E2. Phe97 is critical to binding[13], and is stacked between TyrH58 of the H2 loop and AsnH100g of the H3 loop, while Asp96 hydrogen bonds to SerH52 and SerH53 of E2. (*B*) The H3 loop of E2 bridges the MT-SP1 active site, and makes contacts with the 90's, 140's, and 170's loop of the protease. ArgH100b is bound in the S1 pocket, ArgH100c is bound in the S1' pocket, while ProH100e is bound in the S3 pocket. (*C*) ArgH100b is bound sub-optimally in the S1 pocket. Benzamidine (ball and stick, PDB code 1EAX) adapts a substrate like binding orientation, making a salt bridge with Asp189 at the bottom of the S1 pocket of MT-SP1 (distance of 3.1 Å). By comparison, ArgH100b NH_2 of E2 is at a distance of 4.4 Å from Asp189 Oδ1 of MT-SP1 and alternatively makes a water mediated hydrogen bond of 2.9 Å to Asp189.

Figure 3. Stereoview of 2Fo-Fc map at 2σ of the E2 H3 (blue) interacting with Tyr146 of MT-SP1 (gray). The protease Tyr146 side chain is stacked between the side chains of the antibody TyrH99 and

GlnH100a, and the Tyr146 OH residue forms H-bonds with the backbone nitrogens of ProH100 and GlnH100a, at 3.1 Å and 2.9 Å, respectively

Figure 4. E2 adopts a unique conformation in the MT-SP1 active site. (*A*) When the chloromethyl ketone inhibitor D-FPR-cmk (teal, bound to the serine protease fVIIa, PDB code 2FIR) is overlayed in the MT-SP1 active site, the amino acid side chains are buried in the substrate binding sites, S1 (green), S2 (orange), S3 (light magenta) and S4 (purple). By contrast, E2 inserts ArgH100b into the S1 pocket, but then bends above the catalytic residues and binds the P2' GlyH100d and P3' ProH100e in a reverse orientation in the S2 and S3 residues, respectively. This unexpected conformation (*B*) allows the H3 loop to conform to the unique shape of the MT-SP1 binding cleft and make numerous beneficial interactions in the active site, but prevents the loop from being readily cleaved by the enzyme.

Figure 5. Comparison of E2 with HGFA antibody inhibitor Fab58 (PDB code 2R0K). The HGFA structure was aligned with MT-SP1. (A) Fab58 (heavy chain, orange, light chain, light brown) approaches the protease (gray) active site from a different angle than E2 (heavy chain, magenta, light chain, light magenta). The Fab58 light chain also makes very few interactions with the protease. (B) The heavy chain hypervariable loops of both inhibitors bind in the substrate-binding cleft of the protease. Fab58 (orange) binds the H2 and H1 loops in the S2 and S3 substrate pockets, respectively, while the E2 (magenta) H3 loop also binds in the S1 pocket. Both inhibitors "grab" the protease 90's loop, Fab58 with H1 and H3, E2 with H2 and H3.

Figure 6. SPR binding curves of MT-SP 1 (black) and the catalytically inactive mutant R15A (grey) show a lack of binding by the zymogen to E2. Analysis of binding curves for 100, 200 and 500 nM MT-

SP1 R15A did not yield a reliable fit using the BIAcore Evaluation Software, indicating that changes in RU are due to transient association of the zymogen with the chip surface or general buffer effects.

Table 1: E2 / MT-SP1 Interactions

E2 Residue and CDR Loop	MT-SP1 Residue	Type of Interaction	Distance (Å)	Buried surface area (Å^2)
L1 SerL30	Pro173	Hydrophobic	3.7	27
L1 TyrL32	Pro173	Hydrophobic	4.2	66
L3 GlyL92	Gln174	Hydrophobic	3.9	18
L3 AsnL93 Oδ2	Gln174 Oε1	H-bond	3.5	28
L3 TyrL96	Phe97	Hydrophobic	4.0	18
H1 ThrH28 Oγ1	Arg60C NH1	H-bond	3.1	60
H1 SerH30 Oγ	Arg60C N	H-bond	3.0	34
H1 SerH31 N	Asp60D Oδ1	Polar	3.6	17
H1 AlaH33	Phe97	Hydrophobic	3.8	12
H2 SerH52 Oγ	Asp96 Oδ1	H-bond	2.7	28
H2 SerH53 N	Asp96 Oδ2	H-bond	3.2	46
H2 SerH56 Oγ	Asn95 Nδ2	H-bond	2.7	41
H2 TyrH58	Phe97	Hydrophobic	3.3	60
H2 TyrH58 OH	Asn95 Nδ2	H-bond	3.2	
H3 TyrH99	Tyr146	Hydrophobic	3.5	121
H3 TyrH99 OH	Gln221a Nε2	H-bond	3.0	
H3 ProH100 N	Tyr146 OH	H-bond	3.1	5
H3 GlnH100a N	Tyr146 OH	H-bond	2.9	82
H3 ArgH100b NH2	Ser190 Oγ	H-bond	3.3	187
H3 ArgH100b NH1	Ser190 O	H-bond	3.2	
H3 ArgH100c NH2	His57 O	Polar	3.6	153
H3 GlyH100d	Phe99	Hydrophobic	3.7	29
H3 ProH100e	Trp215	Hydrophobic	3.5	106
H3 ProH100e	Phe99	Hydrophobic	4.0	
H3 GlnH100f N	Phe97 O	H-bond	3.1	22
H3 AsnH100g	Phe97	Hydrophobic	3.5	85
H3 AsnH100g Nδ2	Gln174 Oε1	H-bond	2.9	
H3 ValH100h	Gln175	Hydrophobic	3.7	50

Buried surface area determined by PISA[27].

Table 2: Data Collection and Refinement Statistics

	E2 / MT-SP1
Data collection	
Space group	P $2_12_12_1$
Cell dimensions	
a, *b*, *c* (Å)	48.3, 163.1, 201.2
α, β, γ (°)	90, 90, 90
Resolution (Å)	127-2.18 (2.3-2.17)
No. Reflections	774,451
No. Reflections (unique)	74,977
R_{merge}	0.091 (0.569)
$I / \sigma I$	7.5 (1.7)
Completeness (%)	89% (77%)
Redundancy	3.0 (2.5)
Refinement	
Resolution (Å)	85-2.18 (2.23-2.17)
No. reflections	74,828 (4,314)
R_{work} / R_{free}	22.3 / 26.7
No. atoms	
Protein	10,226
Ligand/ion	62 (2 Sulfates, 13 ethylene glycol)
Water	824
B-factors	29 Å^2
Protein	41.8
Ligand/ion	51.2
Water	38.8
R.m.s. deviations	
Bond lengths (Å)	0.02
Bond angles (°)	1.45
Ramachandran Plot	
Favored regions (%)	96.5
Allowed regions (%)	99.9

Values in parentheses are for highest-resolution shell.
Test set was 7.5% of total reflections.

Figure 1

Click here to download high resolution image

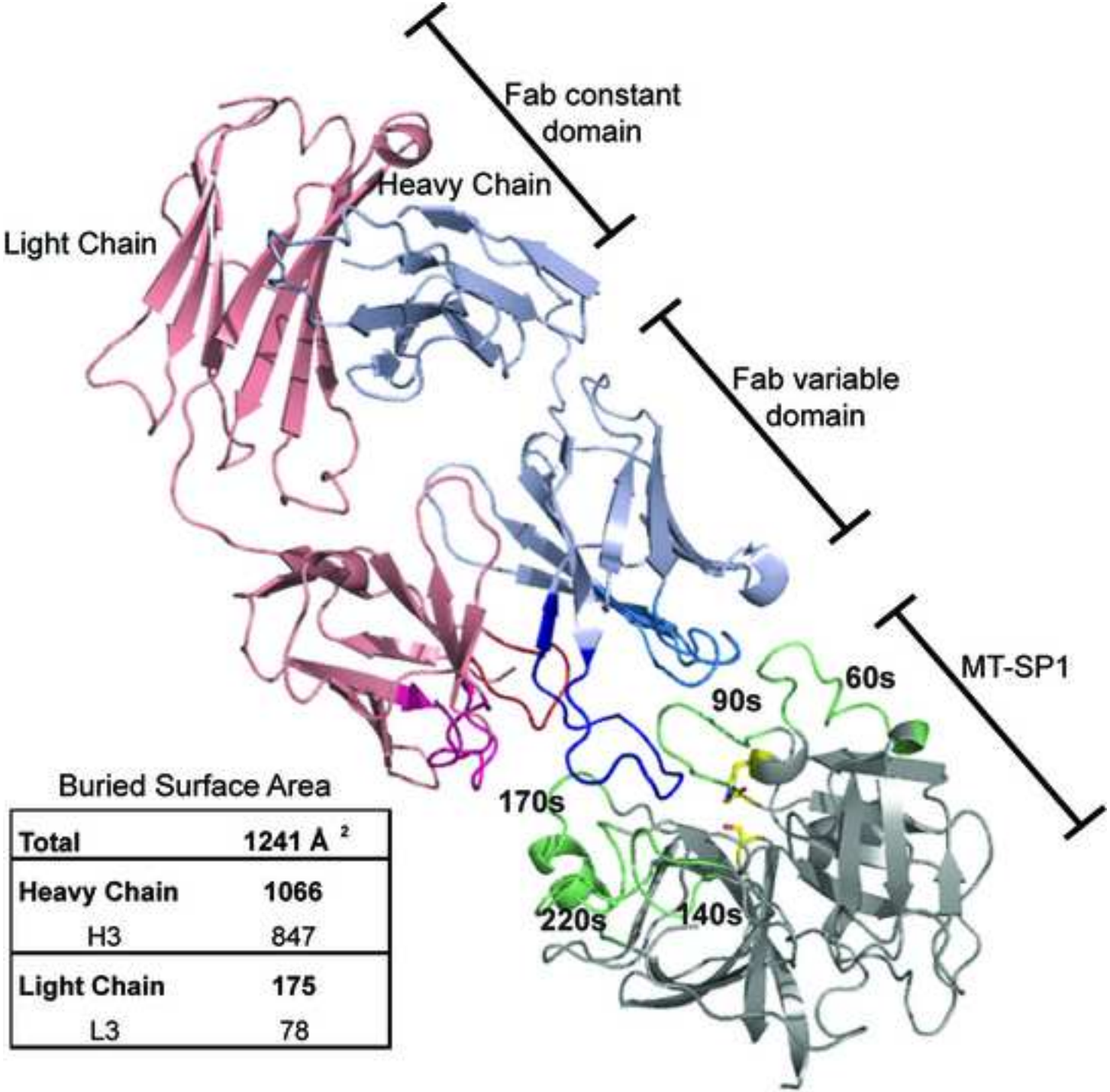

Buried Surface Area

Total	**1241 Å ^{2}**
Heavy Chain	**1066**
H3	847
Light Chain	**175**
L3	78

Figure 2

Click here to download high resolution image

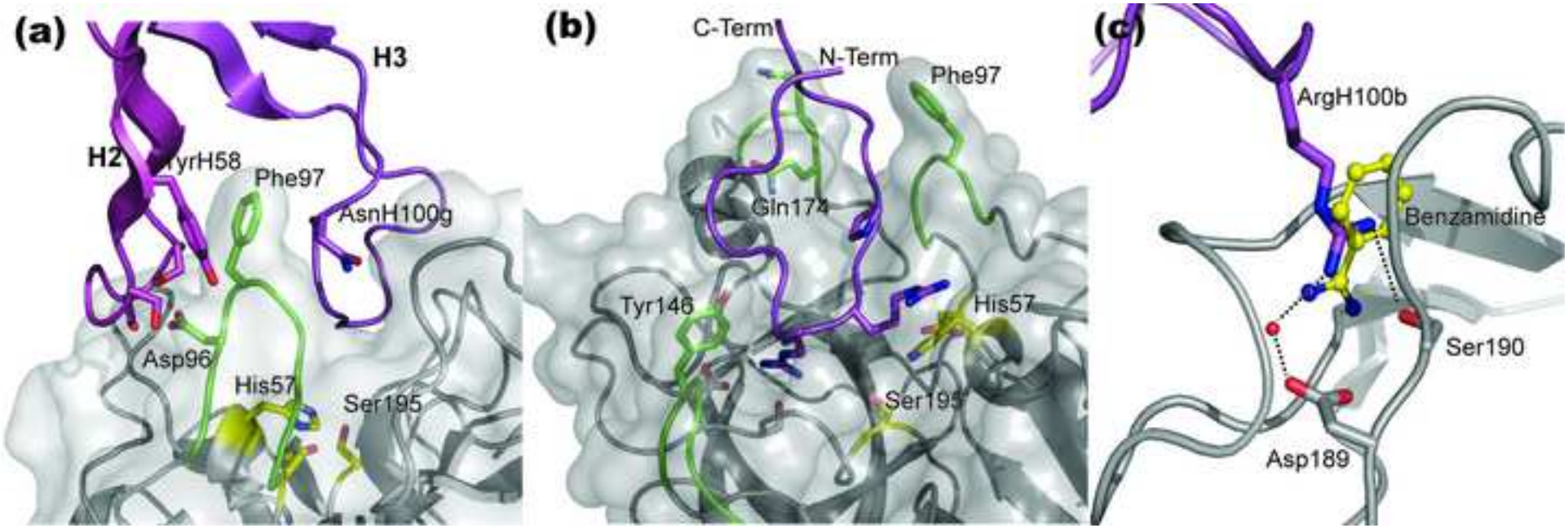

Figure 3

Click here to download high resolution image

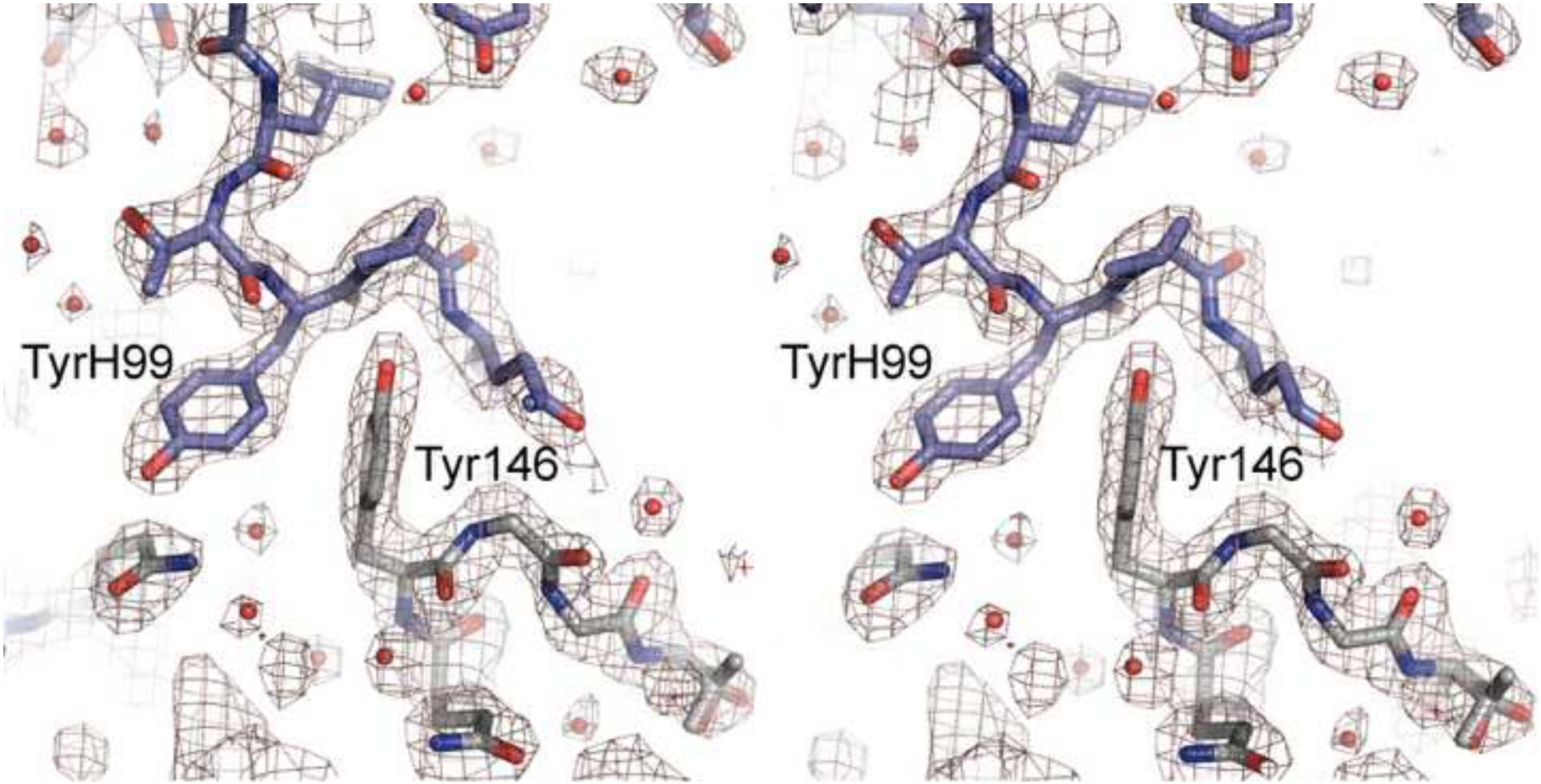

Figure 4
Click here to download high resolution image

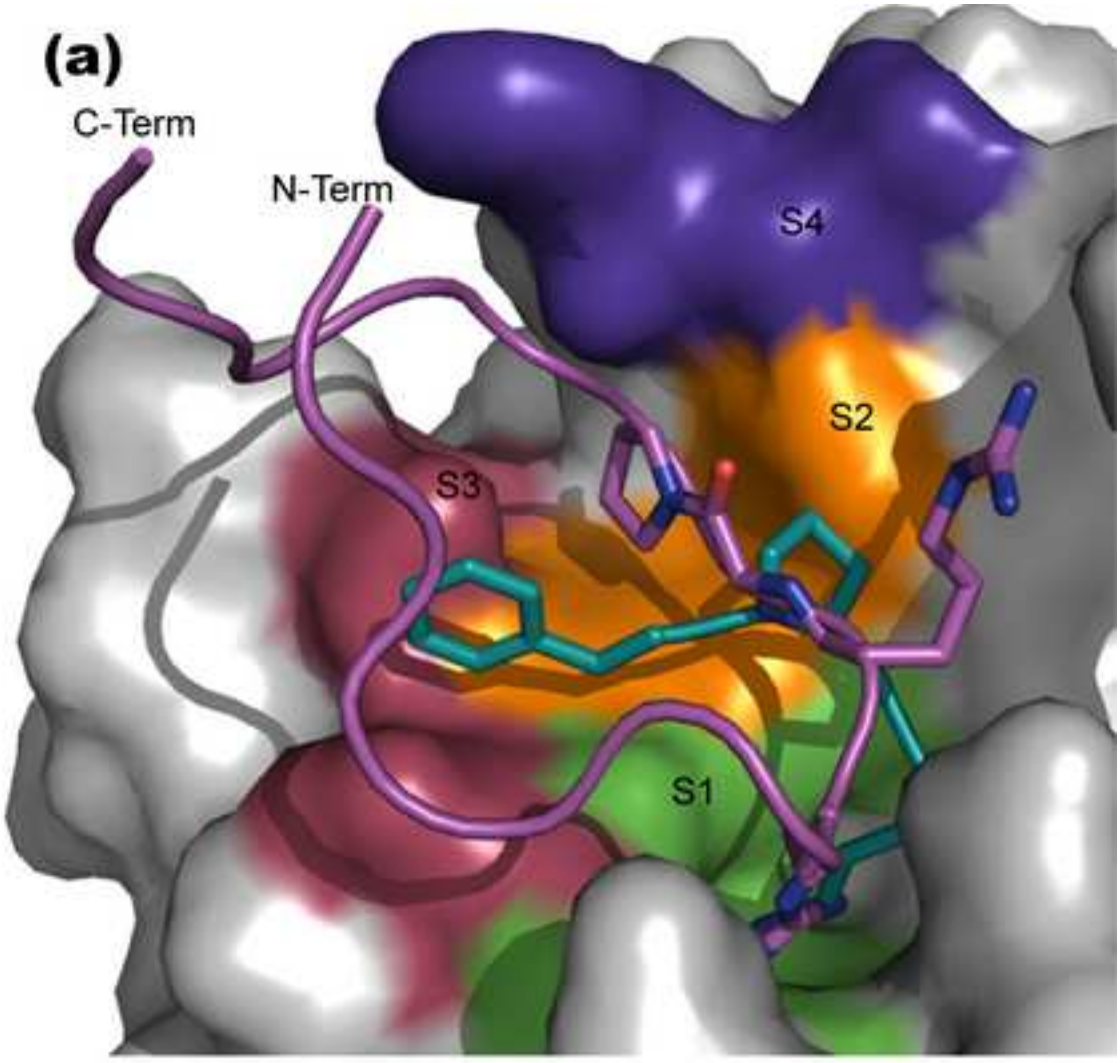

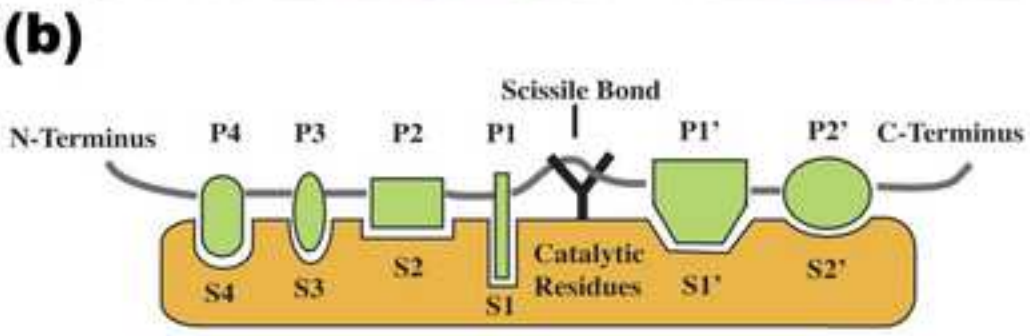

Standard Mechanism Substrate/Inhibitor

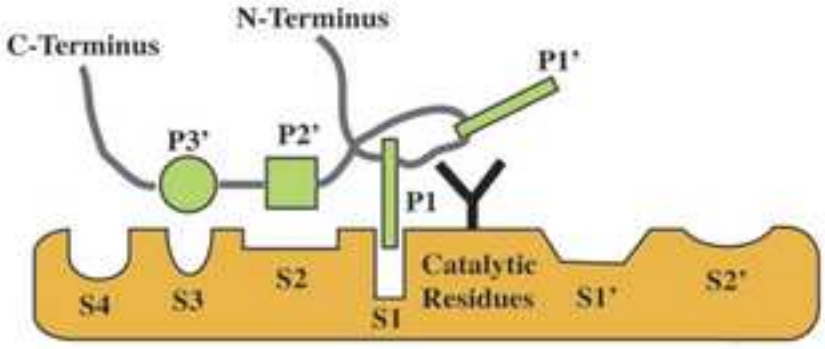

E2 Inhibition of MT-SP1

Figure 5

Click here to download high resolution image

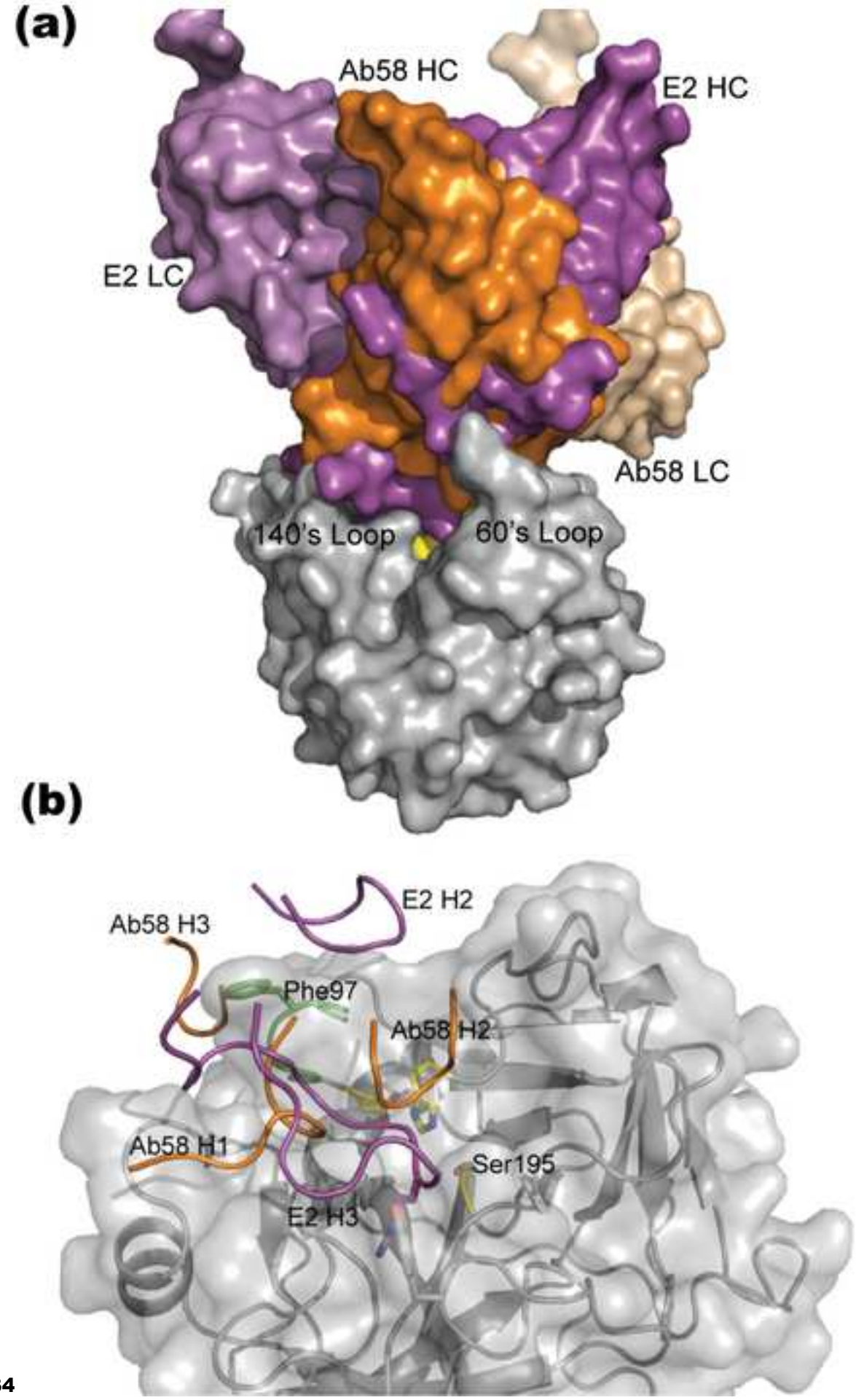

Figure 6

Click here to download high resolution image